*Progress In Electromagnetics Research Letters, Vol. 56, 53–58, 2015*

# A Novel Compact Tri-Band Bandpass Filter Based on Dual-Mode CRLH-TL Resonator and Transversal Stepped-Impedance Resonator

**Hailin Cao[1, 2, *], Mao Yi[1], Huan Chen[1], Jianshuo Liang[1], Yantao Yu[2], Xiaoheng Tan[1], and Shizhong Yang[1, 2]**

**Abstract**—A novel compact tri-band band-pass filter (BPF) with transversal signal interaction concepts, based on composite right/left-handed transmission lines (CRLH-TLs) resonator and parallel stepped impedance resonator (SIR), is presented. The main path is based on a dual-mode CRLH-TL resonator, which exhibits the first two passbands. The secondary path is a SIR, which contributes to the third passband and generates another transmission zero between the first and second passbands simultaneously. The proposed filter has been simulated, fabricated and measured. Both the simulated and measured results show that the filter has a high selectivity with a compact size as small as $0.18\lambda g \times 0.12\lambda g$.

## 1. INTRODUCTION

With the rapid development of multi-band wireless communication, a compact tri-band band pass filter (BPF) with high performance is essential for both the receivers and transceivers in tri-band communication. Various tri-band BPFs have been extensively proposed and studied [1–7]. The most direct method to implement microstrip multi-band BPF is combining multi-sets of different resonators with common input and output [1]. However, these filters generally occupy a large area. On the other hand, dual-mode or multi-mode resonators have been reported to improve the performance of the tri-band BPFs [2, 3], while they always own complicated structures. Another widely used method to design tri-band filters is employing the stub loaded stepped-impedance resonators (SIRs). The loaded stub can properly control the resonant frequencies of the SIRs [4–7]. However, the selectivity of filter with the loaded stub is limited.

Recently, signal-interference techniques have drawn a lot of attention on designing wide-band filters [8–10] and bandstop filters [11]. With a transversal signal path, signal-interaction concept includes multiple transmission zeros to get a high selectivity. However, the circuit size should be further reduced. Left-handed metamaterials have been approved to be able to reduce the dimensions of passive circuits. In [12], a miniaturized SIR BPF based on CRLH-TLs is presented, which has a single passband with a complicated structure.

In this letter, a novel compact tri-band BPF based on signal-interference techniques is proposed. The tri-band BPF incorporates two transmission paths. One path consists of a dual-mode CRLH-TL resonator with a dual passband response. Another path is a SIR, which contributes to the third passband. All the structures are designed and fabricated on the Rogers 4350B with a thickness of 0.762 mm and relative dielectric constant of 3.48. EM simulations are carried out by Ansoft HFSS 13.0. A prototype of the proposed filter has been fabricated and measured.

*Received 4 August 2015, Accepted 8 September 2015, Scheduled 11 September 2015*

* Corresponding author: Hailin Cao (hailincao@cqu.edu.cn).

[1] The Center of Communication and Tracking Telemetering & Command, Chongqing University, Chongqing 400044, P. R. China.

[2] Key Laboratory of Aerocraft Tracking, Telemetering & Command and Communication Ministry of Education, Chongqing University, Chongqing 400044, P. R. China.

## 2. ANALYSIS AND DESIGN OF PROPOSED TRI-BAND BPF

Figure 1 shows the proposed tri-band BPF with two transmission paths (Path I and Path II) based on signal-interaction concept. Path I consists of a dual-mode CRLH-TL resonator with two CRLH-TL units connected by a shorted stub in the middle, while Path II is a SIR. The characteristic impedances for the two microstrip lines at the input/output ports are both $Z_0 = 50\,\Omega$. The equivalent circuit of the periodic CRLH metamaterial cell includes a left-handed series capacitance $C_L$ and a shunt inductance $L_L$, as well as a canonical right-handed series inductance $L_R$ and a shunt capacitance $C_R$. Then, the lumped-element equivalent circuit model of the proposed filter is shown in Fig. 1(b). The inductance $L_L$ at low-frequency $\omega$ and the interdigital capacitance $C_L$ can be approximately obtained by empirical formulas [13], the equations are showed as followed:

$$L_L \approx \frac{Z_c}{\omega}\tan(\beta l), \tag{1}$$

$$C_L \approx (\varepsilon_r + 1)l[(N-3)A_1 + A_2]\,(\mathrm{pF}), \tag{2}$$

$$A_1 = 4.409\tanh\left[0.55\left(\frac{h}{w_s}\right)^{0.45}\right] \bullet 10^{-6}\,(\mathrm{pF/\mu m}), \tag{3}$$

$$A_2 = 9.92\tanh\left[0.52\left(\frac{h}{w_s}\right)^{0.45}\right] \bullet 10^{-6}\,(\mathrm{pF/\mu m}), \tag{4}$$

where $Z_c$, $\beta$ represent the characteristic impedance and the propagation constant; $h$ is the height of the substrate; $l$, $N$ and $w_s$ are the length, number and overall width of the interdigital fingers, respectively. Initial values of $L_L$ and $C_L$ can be calculated by Equations (1)–(4) as a starting value for design.

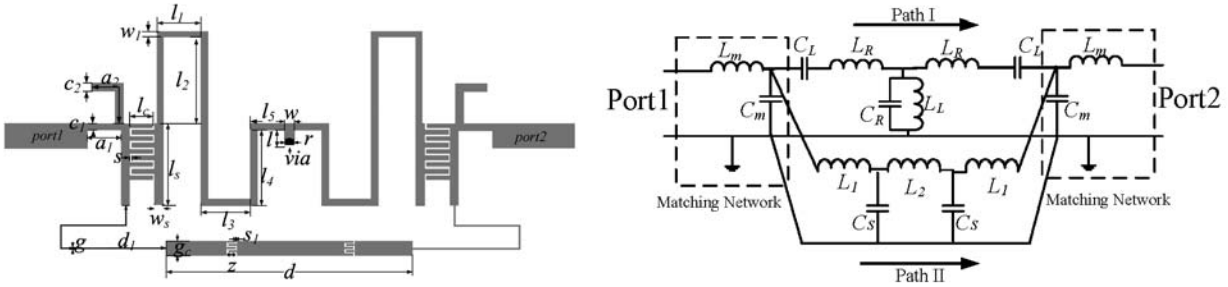


(a) (b)

**Figure 1.** (a) The layout of the proposed filter (Dimensions: $l_s = 6\,\mathrm{mm}$, $l_1 = 2.6\,\mathrm{mm}$, $l_2 = 5.8\,\mathrm{mm}$, $l_3 = 3.1\,\mathrm{mm}$, $l_4 = 5.9\,\mathrm{mm}$, $l_5 = 1.7\,\mathrm{mm}$, $l_c = 1.2\,\mathrm{mm}$, $s = 0.1\,\mathrm{mm}$, $w_s = 0.6\,\mathrm{mm}$, $w_1 = 0.4\,\mathrm{mm}$, $l = 1.2\,\mathrm{mm}$, $w = 1\,\mathrm{mm}$, $a_1 = 2.6\,\mathrm{mm}$, $a_2 = 5.17\,\mathrm{mm}$, $c_1 = 0.5\,\mathrm{mm}$, $c_2 = 0.8\,\mathrm{mm}$, $g = 0.1\,\mathrm{mm}$, $d_1 = 15\,\mathrm{mm}$, $g_c = 1.15\,\mathrm{mm}$, $d = 14\,\mathrm{mm}$, $s_1 = 0.1\,\mathrm{mm}$, $z = 0.15\,\mathrm{mm}$, $r = 0.2\,\mathrm{mm}$. (b) The equivalent lumped element circuit of the proposed filter.

### 2.1. Resonance Characteristic of Dual Mode CRLH Resonator

Path I consists of a dual-mode CRLH-TL resonator with two CRLH-TL units connected by a shorted stub. The behavior of CRLH resonator can be analyzed by odd/even mode analysis because of the symmetrical structure. Figs. 2(a) and 2(b) show the lumped element circuit models for odd/even modes, respectively. The input odd/even impedances $Z_{in\text{-}odd}$ and $Z_{in\text{-}even}$, ignoring the ohmic loss of transmission line, can be expressed as follows:

$$\begin{aligned} Z_{in\text{-}odd} &= j\frac{1-\omega^2(C_{Ro}L_{Lo}+C_LL_{Ro}+C_LL_{Lo})+\omega^4C_{Ro}C_LL_{Ro}L_{Lo}}{\omega C_L(\omega^2L_{Lo}C_{Ro}-1)} \\ &= jL_{Ro}\frac{\omega^4-(\omega_{seo}^2+\omega_{sho}^2+C_LL_{Lo})\omega^2+\omega_{seo}^2\omega_{sho}^2}{\omega(\omega^2-\omega_{sho}^2)} \end{aligned} \tag{5}$$

$$Z_{in\text{-}even} = j\frac{1-\omega^2(C_{Re}L_{Le}+C_LL_{Re}+C_LL_{Le})+\omega^4L_{Le}L_{Re}C_LC_{Re}}{\omega C_L(\omega^2L_{Le}C_{Re}-1)}$$
$$= jL_{Re}\frac{\omega^4-(\omega_{see}^2+\omega_{she}^2+C_LL_{Le})\omega^2+\omega_{see}^2\omega_{she}^2}{\omega(\omega^2-\omega_{she}^2)} \quad (6)$$

where $\omega_{seo}=\frac{1}{\sqrt{C_LL_{Ro}}}$, $\omega_{see}=\frac{1}{\sqrt{C_LL_{Re}}}$, $\omega_{sho}=\frac{1}{\sqrt{C_{Ro}L_{Lo}}}$, $\omega_{she}=\frac{1}{\sqrt{C_{Re}L_{Le}}}$, $\omega_{see}$ and $\omega_{seo}$ represent the series resonant frequencies, $\omega_{she}$ and $\omega_{sho}$ represent the shunt resonant frequencies of the even and odd modes, respectively. It can be seen that there are two resonant peaks in each mode. In order to achieve a passband, two resonant peaks must overlay. At the same time, this requirement also contributes to a high selectivity. The shorted stub in the middle makes the difference resonant frequencies between odd and even mode.

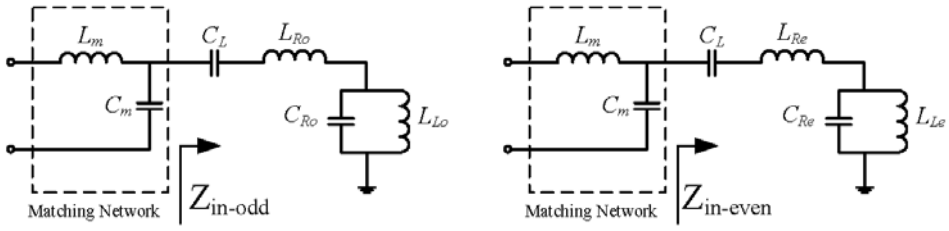


(a) (b)

**Figure 2.** (a) Equivalent circuit in odd-mode. (b) Equivalent circuit in even-mode.

### 2.2. Transmission Response of CRLH Resonator

In order to verify the resonant mechanism of the proposed dual-mode CRLH resonator in Path I, Fig. 3 shows its simulated transmission characteristic with the variation of the shorted-stub length $l$. In the simulations, the width of the shorted-stub is kept constant as 1 mm while the length of it, $l$, is changed from 1.5 to 4.5 mm. As can be seen from Fig. 3, the longer the shorted-stub is, the larger the splitting of the resonant frequency $f_{even1}$ is. This also indicates that the proposed dual-mode CRLH resonator with serial and parallel resonant tank can achieve high selectivity. However, in this case, the results of simulations show that the resonant frequency $f_{odd1}$ of the odd mode is almost unchanged against the variation of the shorted-stub length, which implies that this mode is not perturbed. Every bandwidth of the three passbands is mainly affected by the dimensions of the stub, and secondly affected by the size of interdigital capacitor and port matching network. Adjusting the stub appropriately and fine-tuning other physical parameters, the expected bandwidth can be acquired.

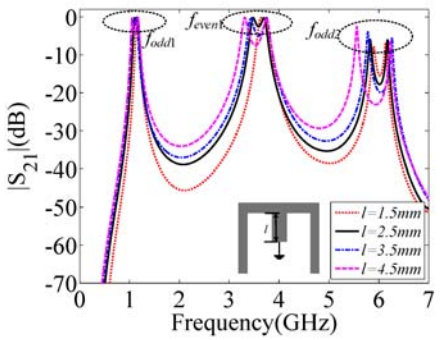


**Figure 3.** Simulated $S_{21}$ of the structure with different $l$.

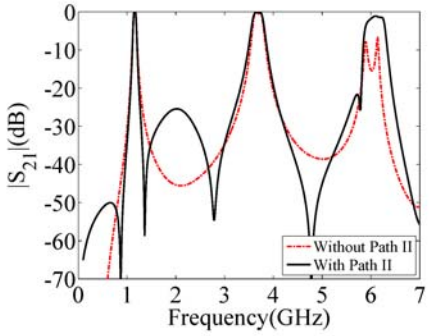


**Figure 4.** Simulated $S$-parameters of the filter with and without the Path II.

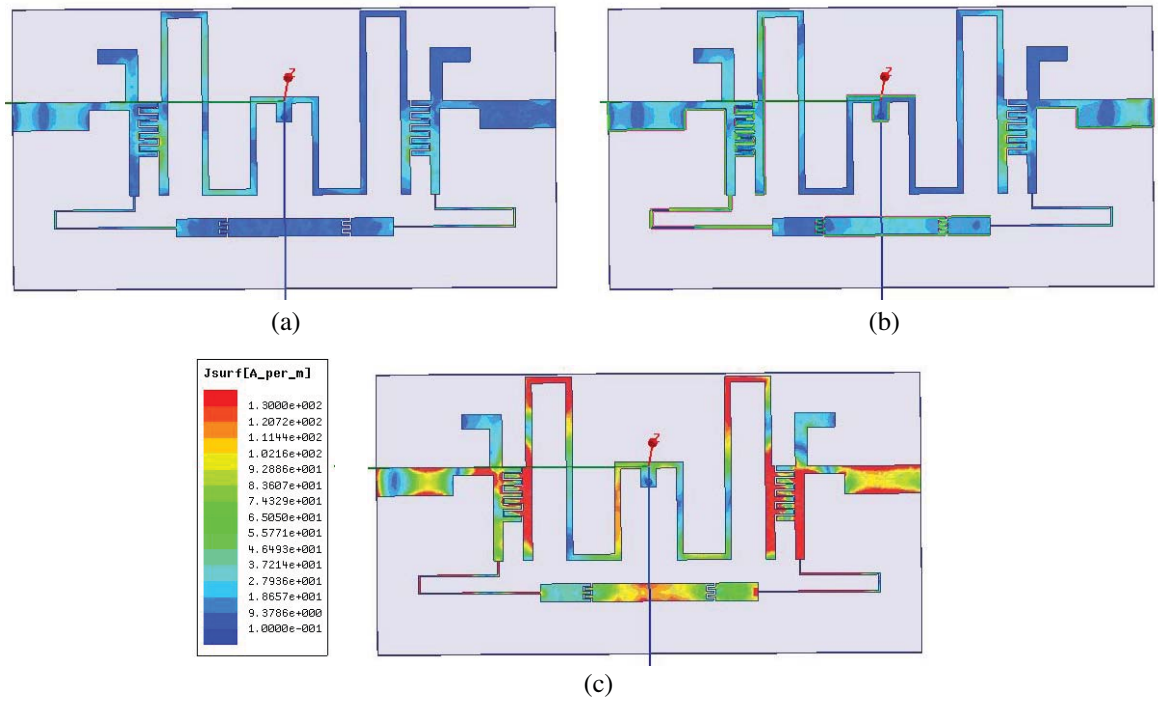


**Figure 5.** The surface current distribution of the proposed filter (a) at the fist (1.16 GHz), (b) the second (3.68 GHz) and (c) the third resonance frequency (6.12 GHz), respectively.

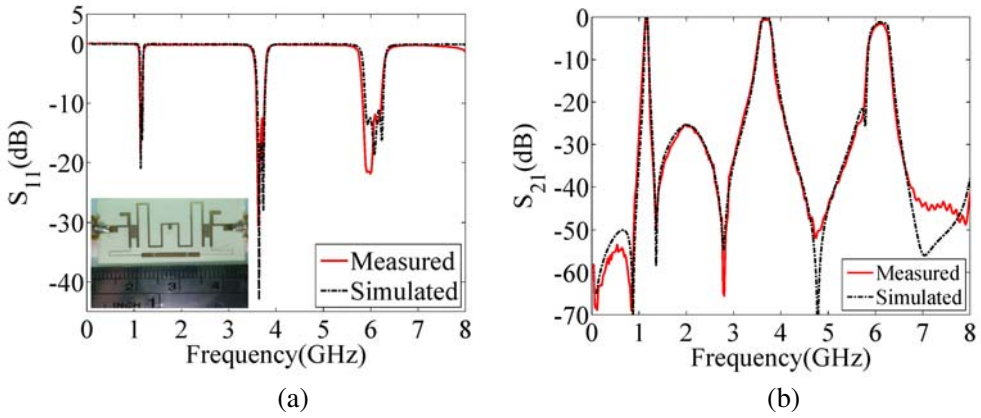


**Figure 6.** Measured and simulated results of the proposed BPF with (a) $S_{11}$ and (b) $S_{21}$.

### 2.3. Proposed Tri-Band Filter with Transversal SIR

To design a tri-band filter and improve the performance of the aforementioned dual-mode CRLH resonator, another path is introduced into the structure, as shown in Fig. 1. Fig. 4 shows the simulated $S$-parameters of the proposed filter with and without the parallel SIR (Path II). Introducing the SIR into Path II has two effects. On one hand, another transmission zero is inserted between the first and second passbands based on transversal signal interaction concept. On the other hand, the third passband is optimized. The surface current distributions of the structure at different resonance frequencies are shown in Fig. 5. It is easy to see that a part of the electromagnetic wave propagates through the parallel SIR, meanwhile, and Path II mainly allows higher frequency signal to pass, which is consistent with the aforementioned impacts of Path II.

## 3. RESULT AND DISCUSSION

The proposed filter is fabricated on a printed circuit board (PCB). The overall size of the filter is 29.5 mm × 19.5 mm ($\approx 0.18\lambda g \times 0.12\lambda g$, where $\lambda g$ is the guided wavelength in the substrate at the central frequency of the first passband). The measured results are extracted by Anritsu 37347C Vector Network Analyzer (VNA), which are shown in Figs. 6(a) and (b). The BPF operates at 1.16 GHz/3.68 GHz/6.12 GHz, with 3 dB factional bandwidths of 5.5%/6.4%/4.5% and insertion loss of 0.16/0.2/1.1 dB, respectively. The return loss is greater than 10 dB in all passbands. It is clear that the response of the fabricated filter agrees well with the simulated ones.

Table 1 shows the performance comparison of the proposed filter with other recently reported tri-band BPFs [1–7]. The proposed filter has a more compact size with high frequency selectivity.

**Table 1.** Performance comparison with reported BPF.

| Filter | 1st/2nd/3rd passbands (GHz) | 3-dB FBW (%) | Circuit size ($\lambda g \times \lambda g$) | Selectivity (20 dB/3 dB) |
|---|---|---|---|---|
| Ref. [1] | 1.8/3.5/5.81 | 7.0/5.0/3.5 | $0.11 \times 0.52$ | 5.56/4.57/3.94 |
| Ref. [2] | 1.95/3.5/5.2 | 8.5/3.7/3.9 | $0.38 \times 0.28$ | 4.83/3.86/2.96 |
| Ref. [3] | 2.4/3.5/5.2 | 4.2/2.9/4.5 | $0.21 \times 0.11$ | 2.58/2.27/2.68 |
| Ref. [4] | 1.25/3.51/6.82 | 24.4/18.3/13.8 | $0.16 \times 0.15$ | 3.61/3.13/1.81 |
| Ref. [5] | 1.575/2.41/3.5 | 5.5/3.8/4.6 | $0.36 \times 0.40$ | 3.46/3.28/2.36 |
| Ref. [6] | 1.93/3.6/4.89 | 19.2/11.6/2.86 | $0.33 \times 0.23$ | 1.89/2.39/5.72 |
| Ref. [7] | 1.37/2.43/3.53 | 4.4/5.9/2.7 | $0.26 \times 0.13$ | 3.32/2.47/1.94 |
| **Ours** | **1.16/3.68/6.12** | **5.5/6.4/4.5** | $0.18 \times 0.12$ | **2.27/2.97/1.95** |

*3-dB FBW (%) = $f_{3\,\mathrm{dB}}/f_0$, Selectivity (20 dB/3 dB) = $\mathrm{BW}_{20\,\mathrm{dB}}/\mathrm{BW}_{3\,\mathrm{dB}}$

## 4. CONCLUSION

This letter presents a novel compact tri-band BPF using a CRLH-TL resonator with a parallel stepped impedance resonator (SIR) based on transversal signal interaction concepts. The proposed filter has been simulated, fabricated and measured. Compared with some recently reported tri-band BPFs, the presented BPF has great improvement on size reduction with high selectivity and simple geometry, simultaneously. The proposed BPF has potential for the multi-band applications in telecommunication, sensor network, and it is useful for enlarging the application of metameterial transmission line.

## ACKNOWLEDGMENT

This work was supported by the National Natural Science Foundation of China under Contract No. 61301120, No. 51377179, No. 61001089, also partly by the Fundamental Research Funds for the Central Universities of CQU (CDJPY12160001).

## REFERENCES

1. Zhang, S.-B. and L. Zhu, "Compact tri-band bandpass filter based on resonators with U-folded $\lambda/4$ coupled-line," *IEEE Microw. Wireless Compon. Lett.*, Vol. 23, No. 5, 258–260, May 2013.
2. Fan, W.-X., Z.-P. Li, and S.-X. Gong, "Tri-band filter using combined E-type resonators," *Electron. Lett.*, Vol. 49, No. 3, 193–194, 2013.

3. Jankovic, N., R. Geschke, and V. Crnojevic-Bengin, "Compact tri-band bandpass and bandstop filters based on hilbert-fork resonators," *IEEE Microw. Wireless Compon. Lett.*, Vol. 23, No. 6, 282–284, Jun. 2013.
4. Xu, J., W. Wu, and C. Miao, "Compact microstrip dual-/tri-/quad-band bandpass filter using open stubs loaded shorted stepped-impedance resonator," *IEEE Trans. Microw. Theory Tech.*, Vol. 61, No. 9, 3187–3199, Sep. 2013.
5. Chen, W.-Y., M.-H. Weng, and S.-J. Chang, "A new tri-band bandpass filter based on stub-loaded step-impedance resonator," *IEEE Microw. Wireless Compon. Lett.*, Vol. 22, No. 4, 179–181, Apr. 2012.
6. Kumar, N. and Y. K. Singh, "Compact tri-band bandpass filter using three stub-loaded open-loop resonator with wide stopband and improved bandwidth response," *Electron. Lett.*, Vol. 50, No. 25, 1950–1952, Dec. 2014.
7. Lan, S.-W. and M.-H. Weng, "A tri-band bandpass filter with wide stopband using asymmetric stub-loaded resonators," *IEEE Microw. Wireless Compon. Lett.*, Vol. 25, No. 1, 19–21, Jun. 2015.
8. Feng, H., J. Zhao, and B. Wang, "Compact microstrip UWB bandpass filter with triple-notched bands and wide upper stopband," *Progress In Electromagnetics Research*, Vol. 144, 185–191, 2014.
9. Feng, W.-J. and W.-Q. Che, "Novel ultra-wideband bandpass filter using shortedcoupled lines and transversal transmission line," *IEEE Microw. Wireless Compon. Lett.*, Vol. 20, No. 10, 548–550, Oct. 2010.
10. Feng, W.-J., W.-Q. Che, Y.-M. Chang, S.-Y. Shi, and Q. Xue, "High selectivity fifth-Order wideband bandpass filters with multiple transmission zeros based on transversal signal-interaction concepts," *IEEE Trans. Microw. Theory Tech.*, Vol. 61, No. 1, 89–97, Jan. 2013.
11. Liu, G. and Y. Wu, "Novel in-line microstrip coupled-line bandstop filter with sharp skirt selectivity," *Progress In Electromagnetics Research*, Vol. 137, 585–597, 2013.
12. Karimian, S. and Z. Hu, "Miniaturized composite right/left-handed stepped-impedance resonator bandpass filter," *IEEE Microw. Wireless Compon. Lett.*, Vol. 22, No. 8, 400–402, Aug. 2012.
13. Caloz, C. and T. Itoh, *Electromagnetic Metamaterials*, 122–125, Wiley, New York, 2005.